

# Observing Disaggregated Cross-Channel NLI Generation in Dispersion-Managed Links

Elliot London, Emanuele Virgillito, Andrea D’Amico, Vittorio Curri

*Politecnico di Torino, Corso Duca degli Abruzzi, 24, 10129, Torino, Italy*

*elliott.london@polito.it*

**Abstract:** We evaluate the generation of the cross-channel interference (XCI) contributor of the nonlinear interference (NLI) using split-step Fourier method (SSFM) simulations, for a variety of dispersion-managed optical links, as part of a disaggregated optical network segment. By comparing these results to the Gaussian noise (GN) model we outline the behavior of the XCI accumulation, observing that this quantity reaches an asymptotic upper bound. This quantity is observed to depend on the residual dispersion within the link, scaling with the parameters of the underlying fiber spans and the transmitted signals.

## 1. Introduction

The majority of backbone networks transmit dual-polarization (DP) and coherent signals that are supported by rapidly-progressing technologies, with the next generation of upgrades being to 400G-ZR+, enabling 64 GBd transmission in a 75 GHz, wavelength division multiplexing (WDM) grid, for total bandwidths of up to 4.8 THz. Conversely, many metro and access networks still make use of fiber links with built-in dispersion compensation in the form of dispersion compensation units (DCUs) and channels transmitting intensity-modulated direct-detected (IMDD) signals. As these latter networks are progressively upgraded to handle the advance of coherent technologies, the topic of managing the quality of coherent signals through dispersion-managed links has become relevant. Concurrently, recent innovations within optical networking are producing a shift towards architectures that enable software-defined networking (SDN) technology, such as wideband and disaggregated network frameworks, in order to maximize network performance. In a disaggregated framework, a multi-vendor approach is permitted, enabling a higher level of flexibility, transmitting coherent lightpaths (LPs) along optical line systems (OLSs), with the signal managed at their termination by open and disaggregated reconfigurable optical add-drop multiplexers (ROADMs) [1].

In order for SDN controllers to establish and evaluate new and existing LPs it is necessary to make use of a quality of transmission (QoT) estimator, or QoT-E. A QoT-E permits the degradation of the signal to be evaluated as it propagates through the LP. Through an OLS, QoT-E is commonly given by the generalized signal-to-noise ratio (GSNR) [2]:

$$\text{GSNR}^{-1} = \text{OSNR}^{-1} + \text{SNR}_{\text{NL}}^{-1}, \quad (1)$$

where the linear and nonlinear contributors to the QoT degradation are given separately as OSNR and  $\text{SNR}_{\text{NL}}$ , respectively. The most major OSNR contributor is the amplified spontaneous emission (ASE) noise that arises from the amplification process, whereas the nonlinear contribution,  $\text{SNR}_{\text{NL}}$ , may in turn be separated into the self-channel interference (SCI) and cross-channel interference (XCI) [3, 4]. A disaggregated approach to  $\text{SNR}_{\text{NL}}$  has previously been demonstrated, whereby the SCI and XCI contributors are separated, enabling individual OLSs within the LP to be evaluated separately. This approach is aided by the calculation of the maximum SCI contribution, also investigated for network configurations that have variable fiber span characteristics, i.e., with fiber lengths changing across two network segments [5]. Applying a disaggregated approach to dispersion managed links, a distinct behavior for the SCI NLI contributor has previously been observed [6], but has not yet been investigated for the XCI contributor.

Within this work we investigate the generation of XCI within a disaggregated network scenario, performing numerical simulations using an implementation of the split-step Fourier method (SSFM) that solves the dual polarization Manakov equation [7], based on an implementation summarized in [8]. We consider a variety of network configurations, emulating various disaggregated network segments that include DCUs that produce different residual dispersion values. These configurations feature a connection between two distinct OLSs, each of which with distinct fibers dispersion values, along with a variety of spectral configurations. The estimated gradient of the accumulated XCI is

compared to analytical values obtained from the Gaussian noise (GN) model [9], in this case implemented using the open-source GNPY library [10].

## 2. Split-Step Fourier Method Simulations

To estimate the XCI contribution in a variety of dispersion-managed scenarios, we perform an extensive set of SSFM simulations using a common framework. We start with the line configuration; as we wish to investigate a realistic, worst-case scenario within a disaggregated optical network, we consider a segment within a disaggregated network, shown in Fig. 1. This consists of two distinct OLSs; the first with 10 spans of fiber of a single, uniform dispersion, followed by 20 spans of a second OLS, with a different uniform dispersion value. All other fiber parameters are set to be equal throughout the campaign; we consider length values of  $L_s = 80$  km, nonlinear coefficients,  $\gamma = 0.00127$ , and loss values,  $\alpha = 0.2$  dB/km. The two distinct chromatic dispersion values considered were  $D = 4$  and  $16$  ps/(nm·km), for the first and second OLSs, respectively, and vice versa. These parameters have been chosen as they correspond closely to common values given by the widely deployed ITU-T G.652D fiber type [11]. As we are interested only in the XCI component, each fiber span is followed by an ideal, transparent amplifier, generating no ASE noise. We remark that, although we operate the amplifiers in a state of transparency, this condition may be relaxed without any loss of generality. A DCU is placed after each amplifier, providing a level of chromatic dispersion compensation with a residual value that is set to a constant and identical value throughout the entire link. The residual dispersion is calculated according to the following relation:

$$D_{RES} = DL_s + D_{DCU}, \quad (2)$$

where  $D_{DCU}$  is the dispersion applied by the DCU. Concerning the spectral information, we consider one channel under test and a single interfering channel within the center of the C-band (193.9 THz), separated by  $\Delta f = 150$  GHz, both with a modulation format of 16-QAM (quadrature amplitude modulation) and a large amount of predistortion applied such that the signal may be considered to be Gaussian prior to transmission, in order to exclude effects due to signal gaussianization [6, 9]. Baud rates,  $R_s$ , of 32 and 64 GBaud have been considered, corresponding to channel bandwidths of 37.5 and 75 GHz, respectively. The signal is generated for each channel, for each polarization, using independent pseudo-random binary sequences (PRBSs) with a 17th degree polynomial, providing a total of  $2^{17}$  bits. The signal is then propagated through the system and received by a coherent digital signal processing (DSP) module, first consisting of a resampling filter, and an ideal analog-to-digital converter (ADC), and a chromatic dispersion compensation (CDC) unit, compensating for the total  $D_{RES}$  accumulated for each passed fiber span. Following this, an adaptive equalizer, and carrier phase estimation (CPE) module are applied, finally calculating the XCI contribution by calculating the error vector magnitude (EVM) of the received signal, at each fiber span, at 1 sample per symbol.

## 3. Results and Analysis

We show selected results from this simulation campaign in Figs. 2a–2d, for fiber dispersion configurations of  $D = [4, 16]$  ps/(nm·km), and vice versa, and  $D_{RES}$  values of 40 and 160 ps/nm. These results are presented in terms of XCI power gradient, defined for a span index  $n$  as:

$$\Delta P_{XCI,n} = P_{XCI,n} - P_{XCI,n-1}, \quad (3)$$

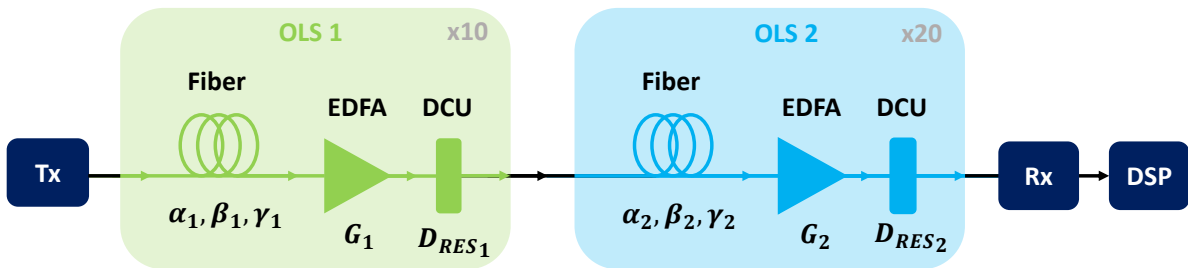


Fig. 1: Schematic of the disaggregated, dispersion-managed optical network segment under investigation in this work.

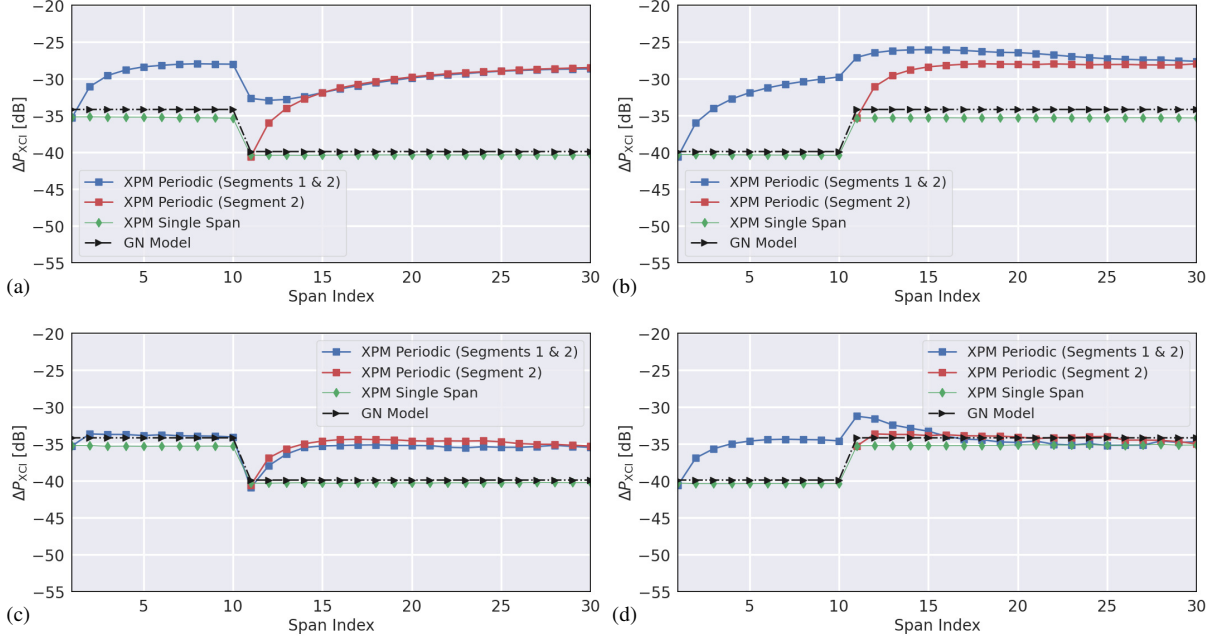


Fig. 2: The NLI accumulation for a disaggregated network segment, given in terms of XCI power gradient versus span index. Included are the simulation results for the entire segment (blue lines), for the final 20 spans (red lines), each span evaluated independently (green lines) and an implementation of the GN model (black dashed lines). The four configurations are as follows; (a):  $D = [4, 16]$ ,  $D_{\text{RES}} = 40$ , (b):  $D = [16, 4]$ ,  $D_{\text{RES}} = 40$ , (c):  $D = [4, 16]$ ,  $D_{\text{RES}} = 160$ , (d):  $D = [16, 4]$ ,  $D_{\text{RES}} = 160$ , in units of  $\text{ps}/(\text{nm}\cdot\text{km})$  and  $\text{ps}/\text{nm}$ , respectively.

where  $P_{\text{XCI},n}$  is the XCI power calculated at the termination of the  $n$ th fiber span. Four approaches to calculating the XCI generation are considered: the XCI is calculated by considering the disaggregated segment in its entirety, given as the blue and red lines, propagating the signal starting from the input of the 1st and 2nd OLSs, respectively. We denote these simulations as the periodic case. The GN model is given by the green line, and in black the XCI given by calculating each fiber span independently is shown, with the latter denoted as the single-span case.

Focusing first upon the single-span case, for all scenarios a good agreement is found between these values and the GN model, demonstrating that an accurate approximation of the XCI is found for an isolated fiber span. Considering Fig. 2a, where  $D_{\text{RES}} = 40 \text{ ps}/\text{nm}$ , for the 1st OLS, we observe that the XCI contribution visibly increases within the first 10 spans, reaching an asymptote. This demonstrates that progressively increasing the total  $D_{\text{RES}}$  within the system causes a progressively larger divergence from the GN model. As the signal passes into the 2nd OLS and the fiber dispersion changes, a decrease in this divergence is initially seen, before a slow accumulation to the same asymptote is observed, with a similar but inverted behavior seen for Fig. 2b. For both of these scenarios, a different initial accumulation is observed when starting propagation from the 2nd OLS, revealing that the  $D_{\text{RES}}$  present within the system induces a coherent effect upon the XCI contribution. This highlights that sole use of the GN model for coherent signals within disaggregated, dispersion-managed network configurations may be insufficient, however, for all configurations, the asymptote is equal for both OLSs. This implies that the stable value depends upon  $D_{\text{RES}}$  and the fibers within the first OLS, and consequently the asymptote may be calculated if the initial configuration of the dispersion-managed section of the network is known.

Focusing next upon Figs. 2c–2d, the same behavior is observed, but with a reduction between the asymptote and the GN model, along with the distance required to reach the asymptotic level. For  $D_{\text{RES}}$  values larger than  $160 \text{ ps}/\text{nm}$ , we observed that the accumulation tends quickly towards the level given by the GN model, whereas for  $D_{\text{RES}}$  values smaller than  $40 \text{ ps}/\text{nm}$ , an increasingly large total length was required to reach the asymptote. Combining the information gleaned from this simulation campaign, the asymptotic value of the XCI accumulation in the presence of residual dispersion arising from partial compensation by a DCU, denoted  $\theta_{\text{XCI}}$  was found to scale with:

$$\theta_{\text{XCI}} \propto \Delta f^2 R_s^2 \beta_1 L_s, \quad (4)$$

where  $\beta_1$  is the chromatic dispersion of the fibers in the first OLS, given a uniform OLS. We remark that this relation bears significant similarity to the behaviour of the SCI accumulation [12], suggesting that these parameters provide an intrinsic characterization of coherent NLI contributions, for both SCI and XCI.

#### 4. Conclusion

Within this work we have presented an investigation of the accumulation of XCI in a variety of dispersion-managed links in a realistic disaggregated optical network segment. We show that this accumulation has a maximum per-span value which depends upon the chromatic dispersion of the first fibers within this segment, and that this effect scales according to a unique combination of intrinsic fiber and transmission parameters. As a result, an upper bound for NLI generation in dispersion-managed links with low residual dispersion values may be found with the use of the GN model, enhanced with knowledge of the maximal XCI generation for the system under configuration.

#### Acknowledgments

This project has received funding from the European Union's Horizon 2020 research and innovation program under the Marie Skłodowska-Curie grant agreement 814276.

#### References

1. N. Sambo, P. Castoldi, A. D'Errico, E. Riccardi, A. Pagano, M. S. Moreolo, J. M. Fabrega, D. Rafique, A. Napoli, S. Frigerio, E. H. Salas, G. Zervas, M. Nölle, J. K. Fischer, A. Lord, and J. P.-P. Gimenez, "Next generation sliceable bandwidth variable transponders," *IEEE Communications Magazine* **53**, 163–171 (2015).
2. V. Curri, "Software-defined wdm optical transport in disaggregated open optical networks," in *2020 22nd International Conference on Transparent Optical Networks (ICTON)*, (IEEE, 2020), pp. 1–4.
3. A. Mecozzi and R.-J. Essiambre, "Nonlinear shannon limit in pseudolinear coherent systems," *Journal of Lightwave Technology* **30**, 2011–2024 (2012).
4. A. Bononi, O. Beucher, and P. Serena, "Single- and cross-channel nonlinear interference in the gaussian noise model with rectangular spectra," *Optics express* **21**, 32254–32268 (2013).
5. E. London, A. D'Amico, E. Virgillito, A. Napoli, and V. Curri, "Modelling non-linear interference in non-periodic and disaggregated optical network segments," *Optics Continuum* **1**, 793–803 (2022).
6. E. Virgillito, A. Castoldi, A. D'Amico, S. Straullu, R. Bratovich, F. M. Rodriguez, A. Bovio, R. Pastorelli, and V. Curri, "Spatially disaggregated modelling of self-channel nli in mixed fibers optical transmission," in *2022 European Conference on Optical Communication (ECOC)*, (IEEE, 2022), pp. 1–4.
7. D. Marcuse, C. Manyuk, and P. K. A. Wai, "Application of the manakov-pmd equation to studies of signal propagation in optical fibers with randomly varying birefringence," *Journal of Lightwave Technology* **15**, 1735–1746 (1997).
8. D. Pileri, M. Cantono, A. Carena, and V. Curri, "Ffss: The fast fiber simulator software," in *2017 19th International Conference on Transparent Optical Networks (ICTON)*, (IEEE, 2017), pp. 1–4.
9. P. Poggiolini, G. Bosco, A. Carena, V. Curri, Y. Jiang, and F. Forghieri, "A simple and effective closed-form gn model correction formula accounting for signal non-gaussian distribution," *Journal of Lightwave Technology* **33**, 459–473 (2014).
10. A. Ferrari, M. Filer, K. Balasubramanian, Y. Yin, E. Le Rouzic, J. Kundrat, G. Grammel, G. Galimberti, and V. Curri, "Gnpy: an open source application for physical layer aware open optical networks," *Journal of Optical Communications and Networking* **12**, C31–C40 (2020).
11. A. Ferrari, A. Napoli, J. K. Fischer, N. Costa, A. D'Amico, J. Pedro, W. Forysiak, E. Pincemin, A. Lord, A. Stavdas *et al.*, "Assessment on the achievable throughput of multi-band itu-t g. 652. d fiber transmission systems," *Journal of Lightwave Technology* **38**, 4279–4291 (2020).
12. A. D'Amico, E. London, E. Virgillito, A. Napoli, and V. Curri, "Quality of transmission estimation for planning of disaggregated optical networks," in *2020 International Conference on Optical Network Design and Modeling (ONDM)*, (IEEE, 2020), pp. 1–3.